ELSEVIER

Biochimica et Biophysica Acta 1467 (2000) 380–394

BIOCHIMICA ET BIOPHYSICA ACTA
BBA

www.elsevier.com/locate/bba

Spin-labeling study of membranes in wheat embryo axes. 1. Partitioning of doxyl stearates into the lipid domains

Ekaterina A. Vishnyakova [a], Andres E. Ruuge [a], Elena A. Golovina [b], Folkert A. Hoekstra [c], Alexander N. Tikhonov [a,*]

[a] *Department of Biophysics, Faculty of Physics, M.V. Lomonosov Moscow State University, Moscow 119899, Russia*
[b] *K.A. Timiryazev Institute of Plant Physiology, Russian Academy of Sciences, Moscow 127276, Russia*
[c] *Laboratory of Plant Physiology, Department of Plant Sciences, Wageningen University, Wageningen, The Netherlands*

Received 1 December 1999; received in revised form 1 May 2000; accepted 11 May 2000

Abstract

The interaction of lipid soluble spin labels with wheat embryo axes has been investigated to obtain insight into the structural organization of lipid domains in embryo cell membranes, using conventional electron paramagnetic resonance (EPR) and saturation transfer EPR (ST-EPR) spectroscopy. Stearic acid spin labels (*n*-SASL) and their methylated derivatives (*n*-MeSASL), labelled at different positions of their doxyl group ($n = 5$, 12 and 16), were used to probe the ordering and molecular mobility in different regions of the lipid moiety of axis cell membranes. The ordering and local polarity in relation to the position of the doxyl group along the hydrocarbon chain of SASL, determined over the temperature range from −50 to +20°C, are typical for biological and model lipid membranes, but essentially differ from those in seed oil droplets. Positional profiles for ST-EPR spectra show that the flexibility profile along the lipid hydrocarbon chain does exist even at low temperatures, when most of the membrane lipids are in solid state (gel phase). The ordering of the SASL nitroxide radical in the membrane surface region is essentially higher than that in the depth of the membrane. The doxyl groups of MeSASLs are less ordered (even at low temperatures) than those of the corresponding SASLs, indicating that the MeSASLs are located in the bulk of membrane lipids rather than in the protein boundary lipids. The analysis of the profiles of EPR and ST-EPR spectral parameters allows us to conclude that the vast majority of SASL and MeSASL molecules accumulated in embryo axes is located in the cell membranes rather than in the interior of the oil bodies. The preferential partitioning of the doxyl stearates into membranes demonstrates the potential of the EPR spin-labelling technique for the in situ study of membrane behavior in seeds of different hydration levels.

Keywords: Doxyl stearate spin label; Embryo axis; Electron paramagnetic resonance; Membrane; Saturation transfer electron paramagnetic resonance; Wheat seed

1. Introduction

There are several biophysical approaches based on spectroscopic techniques (nuclear magnetic resonance spectroscopy, electron paramagnetic resonance (EPR) spectroscopy and Fourier transform infrared

Abbreviations: EPR, electron paramagnetic resonance; MeSASL, methyl ester of stearic acid spin label; SASL, stearic acid spin label; ST-EPR, saturation transfer EPR

* Corresponding author. Fax: +7-095-9391195;
E-mail: tikhonov@antbio.phys.msu.su

0005-2736/00/$ – see front matter
PII: S0005-2736(00)00234-0

spectroscopy (FTIR) [1–3]) that can be used to study the dynamic characteristics of seed membranes and their structural changes, for example, during seed ageing. Despite valuable information that can be obtained by these approaches, each method faces specific difficulties with the adequate interpretation of experimental results. The main problem in studying the physical and chemical properties of membranes in such a complex system as an embryo axis is the difficulty in attributing the measured integral parameters to certain intracellular domains. FTIR spectroscopy has been successfully used to investigate molecular interactions in different biological tissues (see [4]). This technique enables an in situ analysis of lipids and proteins in hydrated and dry desiccation-tolerant cells by monitoring specific molecular vibrations. However, FTIR spectroscopy often has difficulties when it is applied to the study of seed membranes, because of the interference from the IR vibrations of lipid molecules located in oil bodies [5].

EPR spectroscopy of lipid soluble spin labels is widely used to study model and biological membranes (see reviews in [2,6–9]). Using a set of spin labels that have different chemical structures, an experimenter has the possibility to probe different lipid domains in an intact cell. Stearic acid spin labels (SASLs; doxyl stearates) are the most popular spin probes for testing model and biological membranes [2,6–15]. They have an obvious advantage for analyzing membrane structures in seeds. As amphiphilic molecules, doxyl stearates are to a certain extent soluble in water and can easily incorporate into embryo axis cells [15]. It also has been demonstrated that 5-SASL molecules (stearic acid with the doxyl group at the 5th position), when added to a suspension of different intact mammalian cells, were located in all cellular membranes, being in rapid equilibrium throughout the membraneous system of the cell [12]. The flip-flop of spin-labelled fatty acids and long chain nitroxide esters across the phospholipid bilayers is fast [10,11]. It is therefore reasonable to expect rather uniform partitioning of doxyl stearates or their methylated derivatives into different cell compartments.

In model membranes (and likely in most biological membranes), doxyl stearates tend to partition into lipid domains that are more fluid [2,9]. However, due to the hydrophilic carboxyl group, doxyl stearates can also bind to proteins and/or tend to concentrate in the vicinity of membrane proteins, i.e. in the protein boundary lipids. Spin labels bound to proteins often give EPR spectra similar to those seen when they are in the lipid domains of membranes [9,14]. To discriminate between these two possible locations, it may be attractive to use spin labels with different positions of the doxyl group. For instance, 5-SASL molecules both in a membrane and on a protein show similar spectra of immobilized nitroxide radical, whereas 16-SASL in the membrane gives a much more 'mobile' spectrum than that of 16-SASL tightly bound to the protein [9,14]. By measuring EPR signals from lipophilic (*n*-MeSASL; methyl ester of SASL) and amphiphilic (*n*-SASL) spin labels, one can probe the physical state of membrane bulk lipids and protein boundary lipids, respectively. Using spin label derivatives labelled by the paramagnetic doxyl group at different positions along the hydrocarbon chain, it becomes possible to study the transmembrane profile of lipid ordering and molecular mobility [2,6–9].

Previously, using EPR spectroscopy of lipid soluble spin labels, we have detected structural differences between the membranes of viable and aged, non-viable wheat embryos [15]. In the present work, we investigated the interaction of SASLs and MeSASLs, with the lipid domains (membranes and oil bodies) in wheat embryo axes to gain insight into the structural organization of cell membranes.

2. Materials and methods

2.1. Reagents

5-, 12- and 16-doxyl stearates (5-, 12- and 16-SASL) and their methyl esters (5-, 12- and 16-MeSASL) were obtained from Aldrich and Sigma (see Fig. 1 for chemical formulas).

2.2. Plant material and seed germination

Wheat (*Triticum aestivum L.*) kernels of cv Pryokskaya of the harvest year 1996 were obtained from a Russian regional seed station. All experiments were performed on wheat kernels after 1 to 2.5 years of storage. As in our previous publication [16], we will

refer to these kernels as seeds, in spite of the fact that botanically they are considered fruits. The seeds were maintained in open storage at ambient temperature. The relative humidity of the surrounding air was not controlled.

The percentages of germinated seeds were determined three times using 100 seeds that were placed on moistened filter paper in glass Petri dishes at room temperature over a period of 7 days. Seeds were considered germinated when protrusions reached more than one-half of the seed size. According to this test, the germination capacity of the seeds was $>85\%$.

2.3. Spin-labelling of embryo axes

2.3.1. Hydrated samples

After excision from the kernels, embryo axes were usually soaked in a spin label solution at room temperature (20°C). The incubation solutions were prepared by adding spin labels from a stock solution of spin label in ethanol to distilled water. After the appropriate time of incubation (mostly 40 min, unless indicated), embryo axes were rinsed several times with distilled water and then loaded into open glass tubes (glass capillaries with an internal diameter of 1.2 mm). The capillaries containing hydrated spin-labelled embryo axes were immediately used for EPR measurements. The final concentration of ethanol in the incubation medium did not exceed 2% (v/v). Using the method described in [15,16], we found that the addition of ethanol ($\leq 2\%$ of the total volume) to the incubation medium did not reduce the barrier function of plasma membranes for ferricyanide ions (data not shown). Also, the presence of small amounts of ethanol ($\leq 2\%$) in the soaking medium did not influence the germination capacity.

2.3.2. Dehydrated samples

Dehydrated spin-labelled samples were prepared in two ways: (i) by fast drying the hydrated spin-labelled samples or (ii) by incubating dry embryo axes in heptane containing spin label. In the first case, hydrated samples were placed on filter paper and were then subjected to a stream of warm air for 10 min to achieve dryness, as assessed by the EPR spectral characteristics of 5-SASL (parameter $2T_{\parallel}'$). In the second case, air-dried embryo axes were placed in a 2 mM heptane solution of spin label. After 40 min of incubation, embryo axes were placed on filter paper for 24 h (at 20°C) to allow the heptane to evaporate. EPR measurements demonstrated that all the traces of a signal from the spin label dissolved in heptane had disappeared after 60 min of exposure of the axes to laboratory air.

2.4. Preparation of spin-labelled oil droplets

Dispersed oil droplets were used as a model to characterize the behaviors of spin labels in the bulk of oil bodies. Spin-labelled oil droplets were prepared by the extrusion of a mixture (volume ratio 1:1) of seed oil and distilled water through a 100-nm pore-size polycarbonate filter, using the LiposoFast instrument (Avestin, Canada) in a similar way as described for the preparation of liposomes [17]. The concentration of spin label in the oil–water mixture was 10^{-3} M. The dispersion of bulk oil into small oil droplets suspended in water enhances the surface-to-volume ratio, promoting the incorporation of doxyl stearates from water solution into the oil droplets.

2.5. EPR measurements

A glass capillary containing six spin-labelled embryo axes was inserted into a quartz tube (internal diameter of 3 mm). A small amount of water was added to the central part of the capillary containing the embryo axes to keep them hydrated. The length of the hydrated sample (axes covered by water) was always standard, approximately 5 mm. To avoid evaporation of water from hydrated samples in the course of the EPR measurements at high temperatures, a small amount of distilled water (50 μl) was placed in the bottom of the quartz tube (out of the sensitive zone of the EPR resonator). Due to capillary effects, water came up to the samples, thus keeping the embryo axes in the hydrated state during the EPR measurements. The quartz tube with the sample was then positioned inside the EPR dewar insert of the EPR spectrometer. The EPR spectra were taken with a Varian E-4 or E-109E X-band spectrometer equipped with a variable temperature controller. Spectra were digitized with an AD convertor and then analyzed with a computer, using software specially produced by B.V. Trubitsin [18].

The rotational motion of spin labels in the submicrosecond time-scale was detected by conventional EPR (first harmonic absorption in phase, 100 kHz field modulation). Conventional EPR spectra (designated V_1) were usually measured at a sub-saturating microwave power of 2 mW. To gain accuracy, we repeated the measurements at a microwave power of 10 mW, which was also below the saturating level. The magnetic field scan range was 100 G and the modulation amplitude was about four times smaller than the EPR line width.

Sub-millisecond rotational motion of spin labels was detected by saturation transfer EPR (ST-EPR) (second harmonic absorption out of phase, 50 kHz field modulation). ST-EPR spectra (designated V_2') were recorded with a peak-to-peak modulation amplitude of 5 G and a microwave power of 70 mW, magnetic field scan range was 100 G. The phase was set by the null method [19], at a sub-saturating microwave power of 0.1 mW.

The temperature was monitored with a copper–constantan thermocouple placed inside the sample tube in the vicinity of the embryo axes, just above the active volume of the cavity. The temperature gradient along the sample tube was negligible; the accuracy of determination of the sample temperature was ± 0.5°C.

2.6. Processing the EPR data

2.6.1. Analysis of conventional EPR spectra (V_1)

An empirical order parameter S, obtained from the conventional EPR spectra, was used to measure the mobility of SASL in the lipid domains of the embryo axis cells. To describe the anisotropic motion of nitroxide radicals, we calculated the principal element of the ordering tensor, parameter S_{zz}. According to [20], the order parameter S_{zz} can be calculated from the following formula:

$$S_{zz} = \frac{1}{7}(T_{\parallel}' + 2T_{\perp}' - \sqrt{\left[\frac{1}{7}(T_{\parallel}' + 2T_{\perp}')\right]^2 - 0.46(T_{\parallel}' - T_{\perp}') + 0.6} \qquad (1)$$

where $T_{\parallel}'$ and $T_{\perp}'$ are the experimentally determined outer and inner splitting parameters (measured in Gauss, see Fig. 2). This approximation accounts for differences in the polarity of nitroxide radical environment. In practice, however, one of the splitting parameters, either $T_{\parallel}'$ or $T_{\perp}'$, is often not resolved, thus preventing the use of Eq. 1. The loss of parameter $T_{\parallel}'$ can result from a small anisotropy of spin label rotation, i.e. in the case that rapidly rotating nitroxide radical is positioned in the depth of the membrane bilayer. Therefore, to determine the apparent order parameter S_{app} from the EPR spectra with unresolved splittings, we have also used the equivalent relationships:

$$S_{app} = \frac{T_{\parallel}' - T_0}{T_{\parallel} - T_0} \qquad (2)$$

or

$$S_{app}* = \frac{T_0 - T_{\perp}'}{T_0 - T_{\perp}} \qquad (3)$$

where T_0 is the isotropic hyperfine splitting constant and $T_{\parallel}$ and $T_{\perp}$ are the principal values of the hyperfine tensor for an axially symmetric system [21]. The values of $T_{\parallel}$, $T_{\perp}$ and T_0 can be obtained experimentally from the EPR spectra corresponding to the isotropically rotating ($S=0$) and complete ordering ($S=1$) of nitroxide radicals. For each kind of spin label used in this work, we determined the $T_{\parallel}$ value from the EPR spectra measured at 77 K, assuming that $T/it > T_{\parallel}' \rightarrow T_{\parallel}$ with decreasing temperature. The isotropic splitting constant T_0 was estimated from the EPR spectrum of spin label in embryo axes measured at rather high temperature (≥ 55°C), when the EPR signal explicitly reveals three relatively narrow lines given by almost isotropically rotating radicals.

2.6.2. Analysis of ST-EPR spectra (V_2')

The mobility of spin labels in the sub-millisecond time interval was analyzed using the line-shape parameters of ST-EPR spectra (V_2'). To evaluate the effective rotational correlation time from V_2' spectra, we determined the ratios of low-field line heights (L''/L) and midfield line heights (C'/C). Experimentally measured parameters L''/L and C'/C were compared with the reference ratios obtained by Horvath and Marsh [22] for spin-labelled hemoglobin. Thus, we formally determined two rotational correlation times, $\tau_R(L)$ and $\tau_R(C)$, corresponding to the ratios L''/L

and C'/C, respectively. For the reference curves presented in [22], we have found that the best fitting analytical approximations that can be used to calculate the apparent submillisecond (0.1 μs–1 ms) correlation time, represent the following sigmoid functions:

$$\tau_R(L) = 103.72\left[\frac{(L''/L)-0.134}{2.48-(L''/L)}\right]^{1.599}\ (\mu s) \quad (4)$$

$$\tau_R(C) = 3.564\left[\frac{(C''/C)+1.041}{1.104-(C'/C)}\right]^{1.591}\ (\mu s) \quad (5)$$

It should be noted that the empirical formulas 4 and 5 only provide the formal procedure for evaluating the apparent correlation times. Rigorously speaking, these formulas should be correct only for radicals rotating slowly in an isotropic medium. Therefore, the correlation times $\tau_R(L)$ and $\tau_R(C)$ obtained from Eqs. 4 and 5 may be different if the nitroxide radical moves in anisotropic medium, e.g. in the membrane. In the latter case, however, one can use the ratio $\xi = \tau_R(L)/\tau_R(C)$ as an effective measure of the rotation anisotropy.

2.6.3. Spectrum integration

The relative number N of spin label molecules incorporated into embryo axes was determined by double integrating the digitized conventional EPR spectra $V_1(H)$, recorded at the sub-saturating microwave power $P = 2$ mW:

$$N = \int\int V_1(H)\mathrm{d}^2H, \quad (6)$$

where $V_1(H)$ represents the conventional in-phase, first harmonic, absorption EPR signal.

All the ST-EPR spectra were normalized to the number of radicals, N, in the sample, by dividing each V_2' spectrum by the relative number of spins N determined from the double integral of the conventional V_1 spectrum. The normalized intensity of the phase quadrature, second harmonic, absorption ST-EPR spectrum is defined according to [23] by the following formula:

$$I_{ST} = \frac{1}{N}\int V_2'(H)\mathrm{d}H, \quad (7)$$

where $V_2'(H)$ represents the out-of-phase, second harmonic EPR absorption signal.

3. Results and discussion

3.1. Partitioning of SASLs into embryo cells

Fig. 1 shows the chemical structures of the lipophilic spin labels, derivatives of stearic acid or stearic acid methyl ester, used in this work as probes of membrane structure. These molecules are labelled with the paramagnetic doxyl group at different positions along the hydrocarbon chain of stearic acid (carbons 5, 12 and 16). Amphiphilic doxyl stearates (*n*-SASL) intercalate in membranes [2,6–9]. The carboxyl group of *n*-SASL acts as the anchor that keeps the hydrophilic head of the molecule in the polar headgroup region of the lipid bilayer, while the hydrophobic tail extends downward toward the hydrocarbon core of the membrane. Thus, spectral parameters of oriented doxyl stearates, plotted as a function of the position (n) of the nitroxide group,

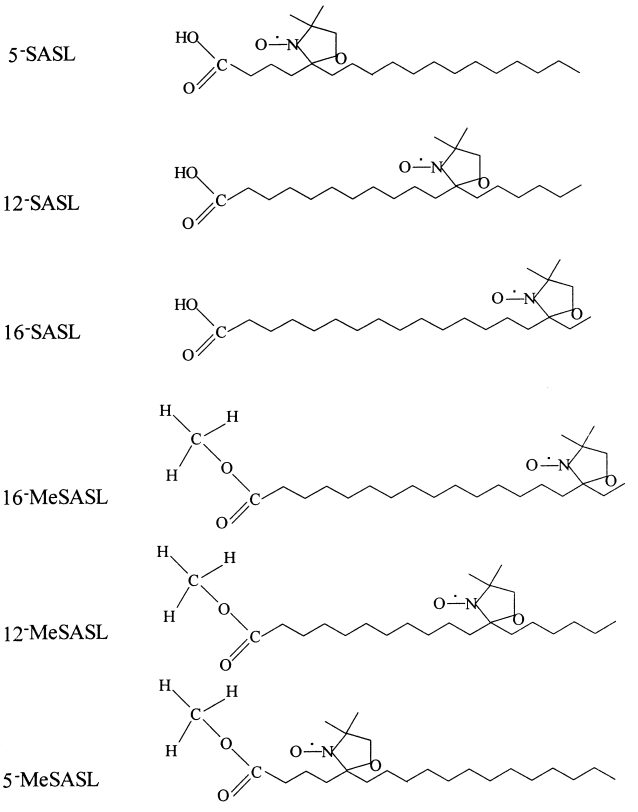

Fig. 1. Chemical structures of spin labels used in this work. Stearic spin labels are intercalated in the membrane with the hydrophilic part (carboxyl group) in the polar headgroup region of the membrane.

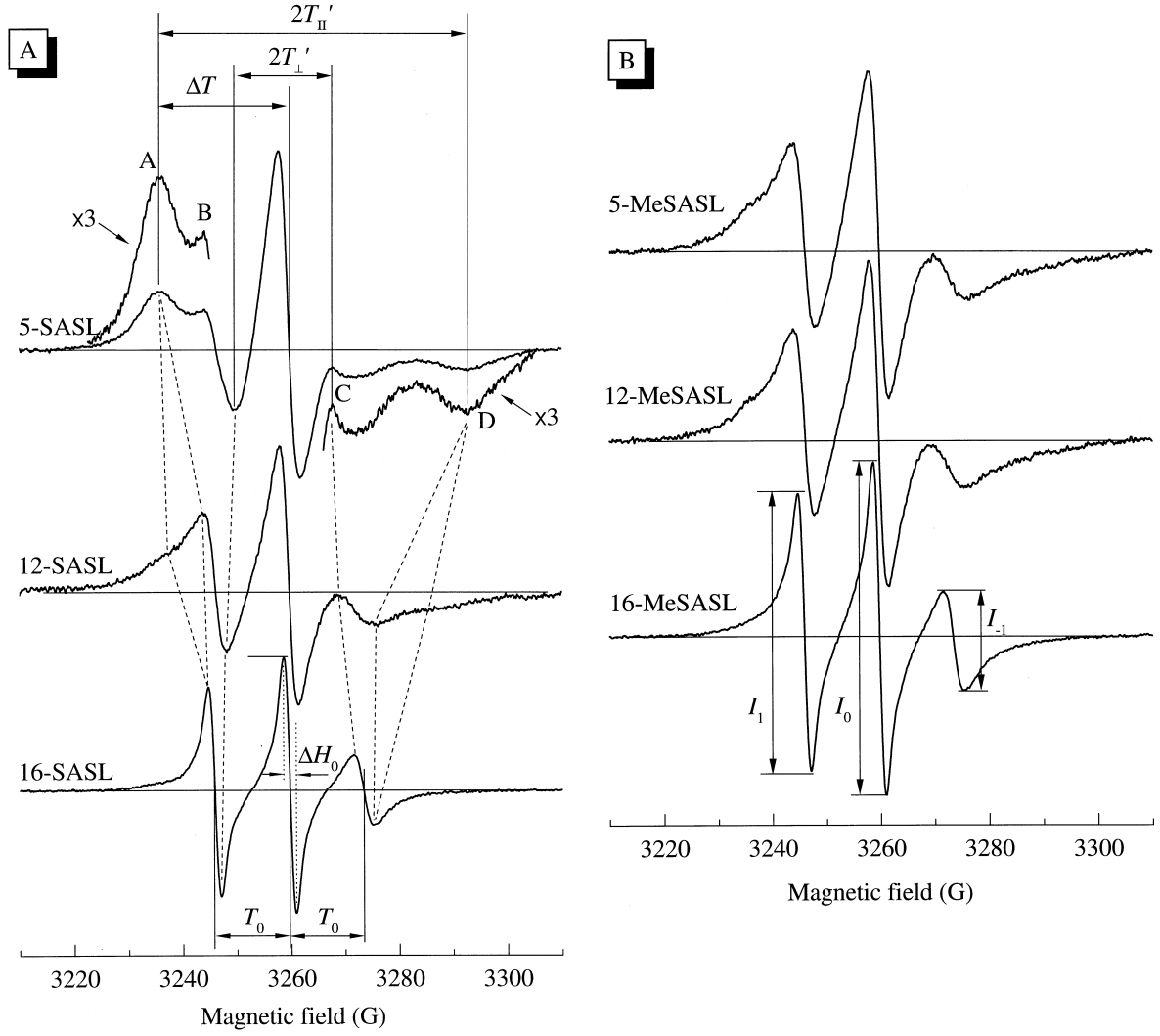

Fig. 2. EPR spectra of doxyl stearic spin labels (A) and their methyl esters (B) in hydrated embryo axes recorded at 20°C. The measured parameters are indicated. The outer wings of the EPR spectra of 5-SASL are also shown as magnified by a factor of 3.

can be used to assay the profiles of ordering and molecular mobility of the acyl chains of membrane lipids. Neutron diffraction measurements in deuterated phosphatidylcholine membranes have demonstrated that the average position of the carbon atoms in the acyl chain can be determined with an accuracy of ±1.5 Å [24]. Meanwhile, the width of the label distribution has been found to increase at the core end of the chain. Owing to the hydrophilic carboxyl group, doxyl stearates can also bind to proteins or concentrate in the boundary lipids of membrane proteins [9,14].

Methyl esters of doxyl stearates are more lipophilic, compared to the free acid derivatives [9]. These spin labels can be used as lipophilic probes for bulk membrane lipids. Methylated spin labels are not supposed to be tightly bound to the surface of the membrane bilayer or attached to membrane proteins, because the electrically neutral methyl group can easily move to the depth of the hydrophobic core of the membrane. Therefore, the location of the nitroxide radicals of *n*-MeSASL in a membrane cannot be directly related to the position of the doxyl group in a spin label molecule [9].

Fig. 2A shows the EPR spectra (at 20°C) from hydrated wheat embryos labelled with different derivatives of *n*-SASL ($n = 5$, 12 and 16). All the spectra presented in Fig. 2A are typical of the EPR signals

given by doxyl stearates located in biological membranes [2]. The EPR signal of 5-SASL reveals distant outer peaks (A and D) and distinct inner peaks (B and C) that are characteristic of nitroxide radicals rotating anisotropically in the lipid bilayer. With deepening of the doxyl group (12-SASL and 16-SASL), the outer peaks A and D move towards the center of the spectrum (the decrease in the $2T_{\parallel}'$ value), while the distance between the inner peaks B and C (parameter $2T_{\perp}'$) becomes greater. These changes indicate that the mobility of the nitroxide radical of *n*-SASL increases with the depth of its location in the membrane.

Fig. 2B shows the EPR spectra (at 20°C) from hydrated wheat embryos labelled with *n*-MeSASL ($n = 5$, 12 and 16). These methylated doxyl stearates gave EPR signals that differed from each other. However, the influence of the doxyl group position on the EPR spectra parameters was not so pronounced (Fig. 2B), as compared with that of *n*-SASL (Fig. 2A). This is likely because the lipophilic *n*-MeSASL molecules can readily move into the lipid bulk of the membrane and do not bind to membrane proteins, thus being able to penetrate into the lipid core of the membrane. Therefore, the location of the nitroxide radicals of the *n*-MeSASLs in the membrane is less determined by the position of the doxyl group along the hydrocarbon chain.

Spectral parameters that we used to analyze the location of spin labels in embryo axes are shown in Fig. 2A. For anisotropically rotating spin labels, the most convenient parameters to characterize the mobility and ordering of nitroxide radicals are the splitting of outer peaks ($2T_{\parallel}'$) [2,6–9,13–15], as well as the position of the low field peak A, relative to the center of the EPR spectrum (parameter ΔT). It is common knowledge that the values of $T_{\parallel}'$ and ΔT increase with decreased rotation of the spin label. In embryo axes, both parameters, $T_{\parallel}'$ and ΔT, were also sensitive to the mobility and ordering of the nitroxide radical. For 5-SASL, the parameters $T_{\parallel}'$ and ΔT usually can be determined over a wide temperature interval. In hydrated axes, the high-field peak D gradually disappeared with the rise of temperature above 30°C, moving towards the center of the spectrum. Meanwhile, the low field peak A remained distinct at temperatures of at least up to 45–50°C (data not shown). That is why we also used the parameter ΔT to characterize the EPR spectra of anisotropically rotating spin labels up to 45–50°C. Another advantage of using the outer peaks A and D, is that these peaks did not superimpose with the relatively narrow lines that might come from weakly immobilized spin labels located in the fluid domains of the cell (e.g. oil bodies [15]). Therefore, the detection of parameters $T_{\parallel}'$ and ΔT also gives the possibility of discriminating between the spin labels located in different lipid domains of cells of embryo axes.

3.2. Time course of spin label incorporation into embryo axis cells

The relative amount N of spin label molecules incorporated into the embryo cells from the incubation medium (aqueous solutions of *n*-SASL, 1 mM) was evaluated by double integrating the conventional EPR spectrum. The value of the double integral (N) increased with incubation time, reaching a steady state level after 100 min of axis soaking (data not shown). For the first 60 min of axes soaking, the accumulation of SASLs inside embryo cells was not accompanied by any essential changes in the shape of the EPR spectrum (the peak-to-peak width of the central line, ΔH_0, and spectrum parameters $2T_{\parallel}'$, $2T_{\perp}'$ and ΔT remained unchanged). This means that accumulation of 5-SASL in embryo axis cells was not accompanied by concentration broadening of the EPR spectrum. After 60 min of incubation we observed a relatively small broadening of the central line with incubation time and certain changes in $2T_{\parallel}'$ and ΔT values (data not shown). The broadening of the EPR signal might occur as a result of frequent collisions of nitroxide radicals at high local concentrations of spin label and/or of certain modifications of the axis cell membranes. To avoid concentration-dependent distortion of the EPR spectra, we usually incubated embryo axes no longer than 45–60 min.

Concentration effects on the shape of the EPR signal were also investigated in experiments with another protocol of labelling, in which axes were incubated for 40 min in solutions with different concentrations of spin label. For 5-SASL, the amount of spin label molecules incorporated into the axes increased with the rise of spin label concentration in the incubation medium, whereas the $2T_{\parallel}'$ remained

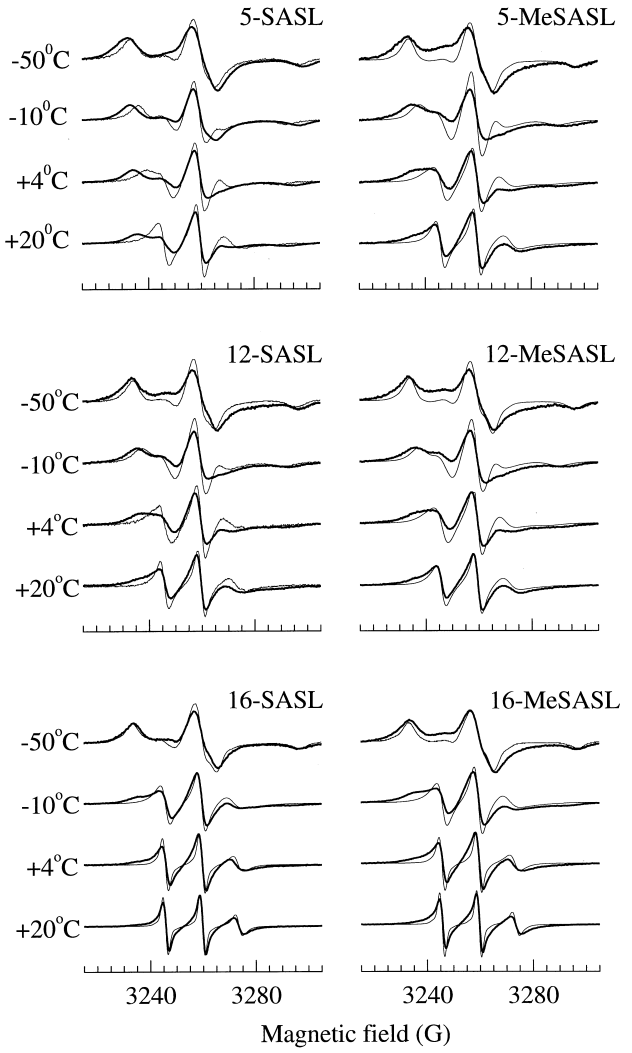

Fig. 3. Effect of temperature on the EPR spectra of spin labels *n*-SASL and *n*-MeSASL ($n = 5$, 12 and 16) in hydrated embryo axes (thick lines) or in seed oil (thin lines). In the latter case, *n*-SASL was dissolved in a suspension of oil droplets; *n*-MeSASL was dissolved in bulk oil.

practically unchanged up to 1 mM of 5-SASL (data not shown). This result demonstrates that under our experimental conditions the EPR spectra were not distorted by concentration broadening.

3.3. Positional profiles of the EPR spectra

An axis represents a complex heterogeneous system with different hydrophobic domains (cell membranes, oil bodies) that could be potent accumulators of amphiphilic and lipophilic spin labels. To characterize the local surroundings of doxyl stearates in embryo axis cells, we consider the positional profiles of the EPR spectral parameters for spin labels located in axes in comparison with a model system of seed oil droplets in suspension. The positional profiles (the dependence of spectral parameters on the position of the doxyl group along the acyl chain) were measured at different temperatures, because it could help to reveal the difference in location of spin labels in axis cells (Fig. 3). Detailed analysis of thermo-induced structural changes in the lipid environment of spin labels in wheat embryo axes will be presented elsewhere [25].

3.3.1. Conventional EPR spectra (V_1)

3.3.1.1. Ordering profiles for nitroxide radicals. Fig. 3 shows the conventional EPR spectra from hydrated wheat embryos labelled with *n*-SASL and *n*-MeSASL ($n = 5$, 12 and 16) recorded at four temperatures (−50, −10, 4 and 20°C). These spectra were compared with the EPR signals of *n*-SASL and *n*-MeSASL dissolved in wheat oil droplets (shown by thin lines). The spectra in Fig. 3 show no evidence of narrow lines that might come from nitroxide radicals located in aqueous surroundings. It is remarkable that all the EPR signals given by spin labels in embryo axes essentially differ from the corresponding signals of spin labels dissolved in oil droplets. The difference in the shape of the EPR spectra became more evident with variation of temperature. For 5-SASL (Fig. 3), spin-labelled embryos always revealed a higher splitting of the outer extreme peaks as compared with the EPR signals from oil droplets. This difference increased with the increase in temperature, demonstrating that over a wide range of temperatures the nitroxide radicals of 5-SASL were more immobilized in embryo cells than in oil droplets. The difference between the EPR signals from embryo and oil was also observed for the lipophilic spin label 5-MeSASL (Fig. 3, right side), indicating that the mobility of MeSASL in the bulk of membrane lipids is lower than in the oil droplets. With the increase in temperature and deeper location of the nitroxide radical into the core of cell membranes ($n = 12$ and 16), the differences between the EPR spectra from embryos and oil became smaller.

To describe the profiles of spin label flexibility in embryo cell membranes, we determined how the or-

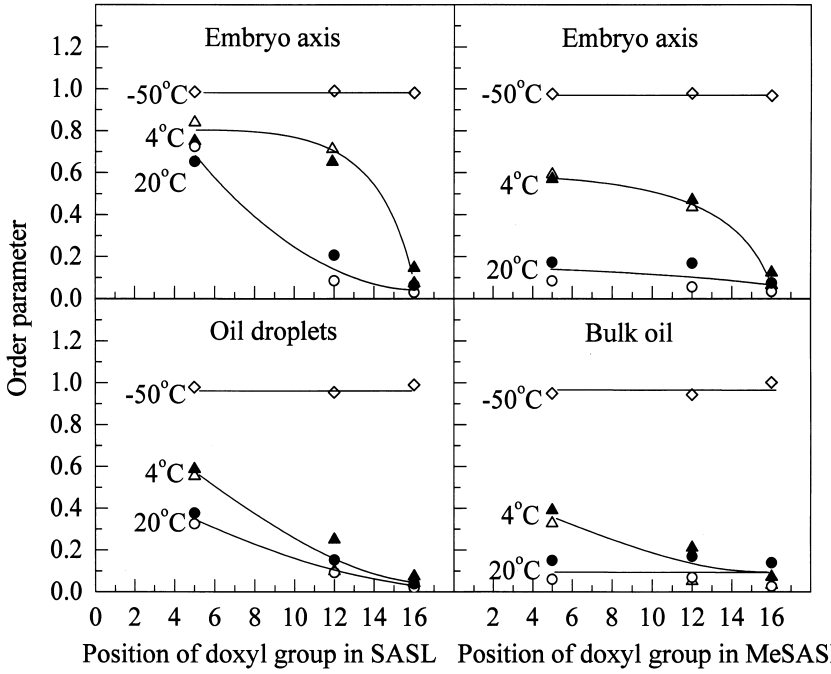

Fig. 4. Top: order parameter S of n-SASL and n-MeSASL in hydrated embryo axes. Bottom: order parameter S of n-SASL in oil droplets and n-MeSASL in bulk oil. The apparent order parameter S_{app} (open symbols) was calculated from the splitting of outer peaks, $2T_{\parallel}'$. For EPR signals measured at 4 and 20°C, the principal value of the ordering tensor, S_{zz} (closed symbols), was calculated according to [20].

der parameter S depended on the position of the doxyl group. When both splitting parameters $2T_{\parallel}'$ and $2T_{\perp}'$ are resolved, it is possible to calculate the order parameter S_{zz} characterizing the ordering of anisotropically rotating nitroxide radicals [2,6–9]. The order parameter S_{zz}, calculated according to Eq. 1, takes into account the polarity of the local surroundings of the nitroxide radicals [20]. At rather low temperatures (≤ -10°C), when parameter $2T_{\perp}'$ was not resolved, we calculated from Eq. 2 the apparent order parameter S_{app}, that can be determined at low temperatures. Fig. 4 compares the profiles of the order parameters S_{zz} (at 4 and 20°C) and S_{app} (at −50, 4 and 20°C) in hydrated spin-labelled axes and oil droplets.

At low temperatures (−50°C), when the mobility of the nitroxide radical is frozen out, the EPR spectra of different spin labels, n-SASL or n-MeSASL ($n = 5$, 12 and 16), in the axes were similar. In this case, the apparent order parameter S_{app}, was practically independent of the position of the doxyl group ($S_{app} \cong 0.98$) and there was also no difference in the values of S_{app} determined for doxyl stearates or their methylated analogs (Fig. 4). With the increase in temperature, the mobility of the nitroxide radicals increased. With heating, the shape of the EPR spectrum became sensitive to the location of the doxyl group in the membrane (Fig. 3); the ordering of nitroxide radicals decreased when the doxyl group was buried more deeply into the membrane (Fig. 4). Both order parameters, S_{zz} and S_{app}, showed similar positional profiles. It is remarkable that EPR spectra of 5-SASL reveal distinct outer (A and D) and inner (B and C) peaks (see also Fig. 2) over the entire temperature interval, indicating that nitroxide radicals undergo fast anisotropic rotation even at room temperature ($S_{zz} \approx 0.75$ at 20°C). Meanwhile, the nitroxide radical of 5-MeSASL was much less ordered as compared with the radical of 5-SASL ($S \approx 0.15$ at 20°C). The flexibility profiles for oil droplets (Fig. 4) showed that spin labels dissolved in oil droplets are much less ordered as compared with those in axis membranes. Note that the ordering of 5-SASL in liquid oil droplets ($S \approx 0.35$ at 20°C) was markedly higher than that of 5-MeSASL ($S \approx 0.1$ at 20°C). This result suggests the anchoring of the hydrophilic carboxyl group of 5-SASL at the water and oil droplet interface.

3.3.1.2. Polarity profiles. Along with the effects of ordering and mobility of the nitroxide radical, the polarity of the surroundings can influence the line shape of the EPR signal. As a measure of polarity, one can use the value of the isotropic hyperfine splitting constant, T_0 (see Fig. 2A). In polar (e.g. aqueous) medium, rapidly and isotropically rotating radicals give characteristic triplet EPR signals with higher values of parameter T_0 than in the hydrophobic environment [2]. For the spin labels *n*-SASL and *n*-MeSASL dissolved in oil droplets, the isotropic splitting constant T_0, determined at rather high temperatures (≥ 20°C), was 13.9 ± 0.1 G, which is typical of nitroxide radicals in hydrophobic surroundings. We obtained a similar value, $T_0 = 13.8 \pm 0.1$ G, for the nitroxide radicals of 12-SASL, 16-SASL and all the methylated spin labels located in embryo axis cells. However, it is practically impossible to find a correct value of T_0 for 5-SASL, because this spin label performs anisotropic rotations in embryo cells even at high temperatures. Bearing this in mind, we have compared the EPR spectra in hydrated and dehydrated axes measured at different temperatures, to detect the polarity profile for doxyl stearates (Fig. 5).

Fig. 5 shows that at room temperature (20°C), the splitting parameter $2T_{\parallel}'$ of 5-SASL in dehydrated axes is higher than in hydrated ones. This result can be explained by a higher rigidity of the membrane lipids in dehydrated embryo cells [15]. At rather low temperatures (≤ -50°C), when the mobility of radicals in both samples was frozen out, the conventional EPR spectra of SASLs lost the sensitivity to slow motion of nitroxide radicals. In this case, the splitting parameter $2T_{\parallel}'$ was independent on the temperature (data not shown). However, the EPR signal in hydrated embryos showed higher splitting of the outer peaks ($2T_{\parallel}' = 66.75$ G), as compared with dehydrated embryos ($2T_{\parallel}' = 64.75$ G). This result can be explained by a different polarity of the nitroxide radical surroundings in hydrated and dehydrated samples. In the case of hydrated phosphatidylcholine, about 10–12 water molecules are bound to each phospholipid headgroup [26,27]. Water molecules in hydrated lipid bilayers influence the hyperfine tensor of nitroxide radicals, leading to an increase of the splitting parameter $2T_{\parallel}'$ [2]. Our comparison of the EPR spectra recorded at low temperature (−50°C) of different SASLs (see Fig. 3) showed that the nitroxide radical of 5-SASL was located in more polar domains than the doxyl groups of the other spin labels. Fig. 6A demonstrates that the splitting parameter $2T_{\parallel}'$, measured at −50°C, decreases with the depth of the doxyl group in the membranes of hydrated cells. This result can be accounted for by differential polarity along the acyl chain of the lipid molecules. Both observations, effect of drying (Fig. 5) and dependence on the doxyl group position (Fig. 6A), indicate that in hydrated embryo axis cells the environment of the nitroxide

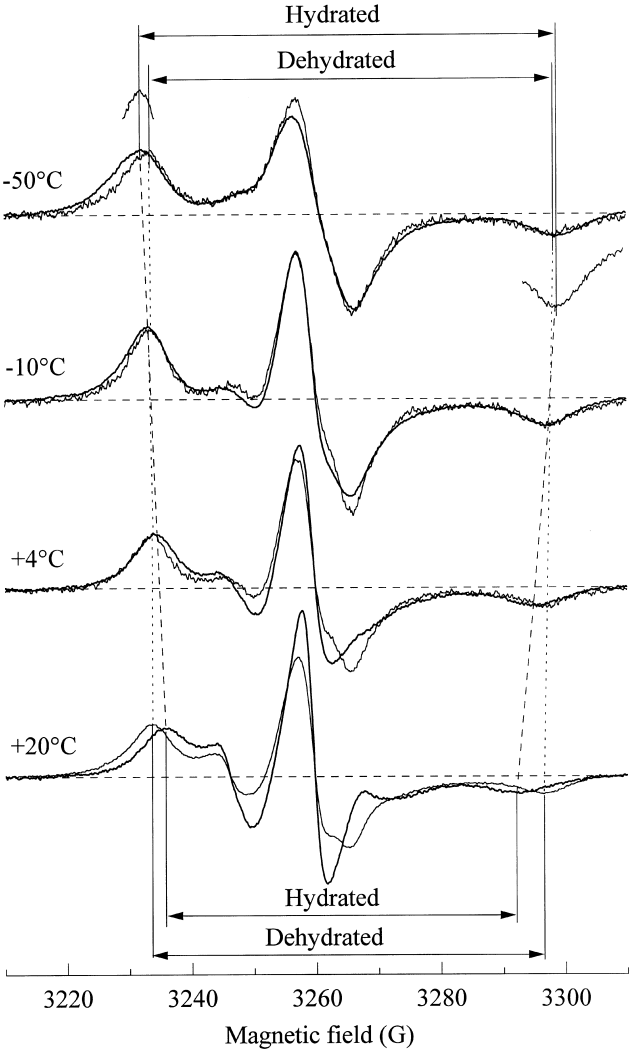

Fig. 5. EPR spectra of 5-SASL in hydrated and dehydrated embryo axes from wheat seeds. Spectra were measured at different temperatures as indicated.

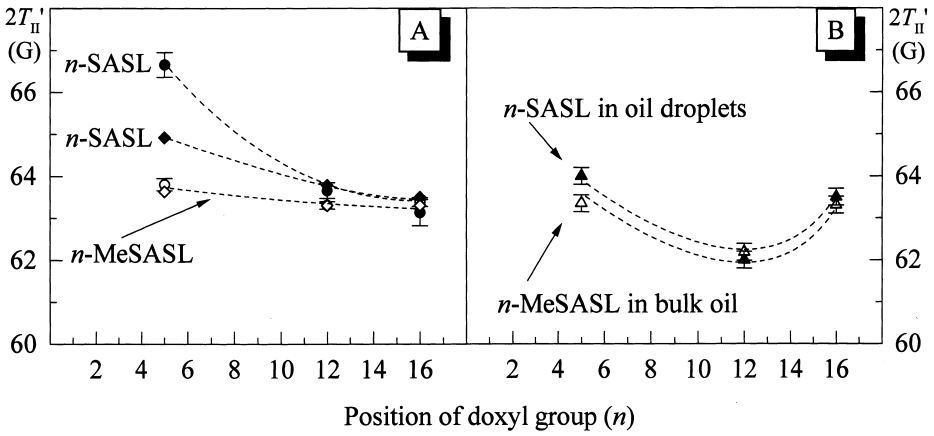

Fig. 6. (A) Spectrum parameter $2T_{II}'$ of *n*-SASL (closed symbols) and *n*-MeSASL (open symbols) measured at −50°C in hydrated (circles) or dehydrated (diamonds) embryo axes. (B) Spectrum parameter $2T_{II}'$ of *n*-SASL or *n*-MeSASL measured at −50°C in a suspension of oil droplets in water (*n*-SASL, closed triangles) or in bulk oil (*n*-MeSASL, open triangles).

radical of 5-SASL is more polar than the surroundings of other doxyl stearates.

In contrast to embryo axis cells, there was no essential difference in the isotropic hyperfine splitting constant T_0 (data not shown) and splitting parameter $2T_{II}'$ (Fig. 6B) between 5-SASL and 5-MeSASL dissolved in oil droplets in water and in bulk oil, respectively. This result means that water molecules from the aqueous bulk of the suspension did not influence the EPR signal given by the nitroxide radicals of 5-SASL located in the oil moiety. This is because water molecules do not penetrate into the oil moiety.

3.3.2. ST-EPR spectra (V_2')

3.3.2.1. Spin-labelled embryo axes. The conventional EPR method loses its sensitivity to the slow (sub-millisecond) motion of nitroxide radicals. Extension of the motional sensitivity of spin labels becomes possible by using ST-EPR spectroscopy (reviewed in [28–33]). The ST-EPR signals from *n*-SASL and *n*-MeSASL in hydrated axes are presented in Fig. 7. These spectra (recorded at −50°C) were normalized to the integral intensities of the corresponding conventional EPR spectra. Since the first publications devoted to ST-EPR spectroscopy of spin labels [28,29], the ratios of the heights of the low field pair of peaks, L''/L, and the central pair, C'/C (see definitions in Fig. 7), were used to calculate the sub-millisecond rotational correlation times. To analyze the low-temperature mobility of nitroxide radicals in embryo axis cells, we have considered these pairs of peaks.

For amphiphilic derivatives of stearic acid (*n*-SASL), the V_2' spectra markedly changed with deeper location of the doxyl group into the membrane. Fig. 7 shows that the ST-EPR spectrum of 5-SASL had a higher value of parameter L''/L than that of 12-SASL or 16-SASL spectra. However, the ratio L''/L changed non-monotonously with deeper location of the doxyl group into the membrane, with a minimum at the position $n = 12$ (Fig. 8). Methylated spin labels (*n*-MeSASL) displayed a positional profile which differed from that of stearic acids: the ratio L''/L had about the same values at the positions $n = 5$ and $n = 12$, but became greater at the position $n = 16$ (Fig. 8A). Methyl ester derivatives of spin labels gave ST-EPR spectra with a smaller value of parameter L''/L, as compared with the corresponding stearic acids. This result means that nitroxide radicals of lipophilic spin labels, including 5-MeSASL, have a higher degree of rotational freedom than the amphiphilic *n*-SASL spin labels. Concerning the ratio C'/C, there was no essential difference between stearic acids and their methylated analogs.

Fig. 8B demonstrates the positional profiles of the apparent rotational correlation times $\tau_R(L)$ and $\tau_R(C)$, calculated from the height ratios L''/L and C'/C, respectively. The positional profile for $\tau_R(L)$ indicates that at low temperatures the mobility of nitroxide radicals in the core of the membrane is several times higher than in the headgroup region of the membrane (5-SASL). It should be noted, how-

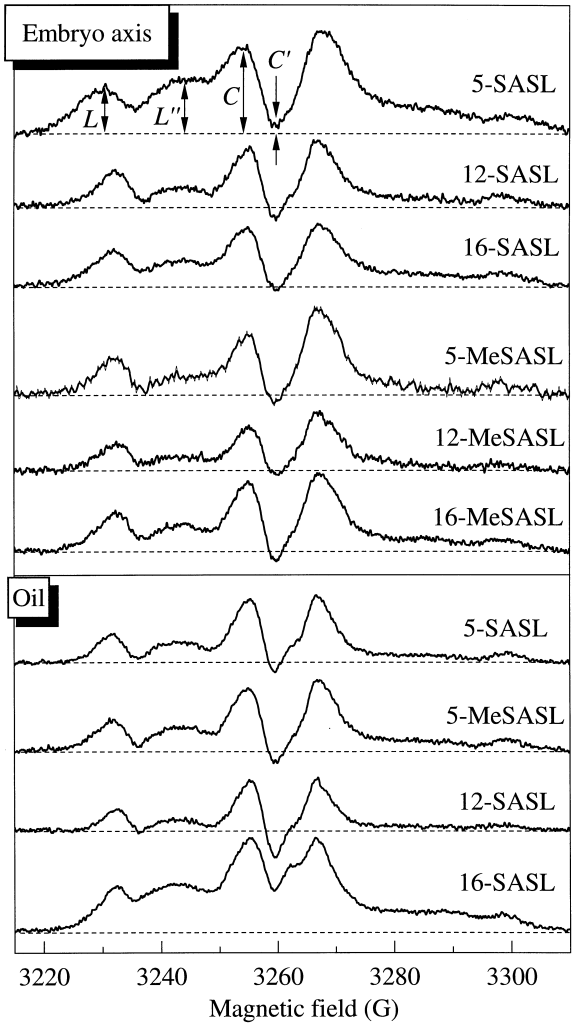

Fig. 7. Top: ST-EPR spectra of doxyl stearic spin labels (5-, 12- and 16-SASL) and their methyl esters (5-, 12- and 16-MeSASL) in hydrated embryo axes. Bottom: ST-EPR spectra of doxyl stearic spin labels (5-, 12- and 16-SASL) in oil droplet suspension and ST-EPR spectrum of 5-MeSASL in bulk oil. All spectra were recorded at −50°C. Spectra were normalized to the relative number of nitroxide radicals in each sample as determined from the double integrals of relevant conventional EPR spectra.

ever, that the apparent correlation time $\tau_R(L)$ essentially differed from $\tau_R(C)$. The values of $\tau_R(L)$ fell in the interval 10–100 μs, while the $\tau_R(C)$ values were about one order of magnitude smaller. The difference in the correlation times $\tau_R(L)$ and $\tau_R(C)$ reflects the anisotropic character of the spin label rotation. The local motion of a doxyl stearate molecule in the membrane could be described by two correlation times, $\tau_\parallel$ and $\tau_\perp$, where $\tau_\parallel$ characterizes the rotation of the spin label about its long axis, and $\tau_\perp$ is related to the rotational motion of this axis with respect to the membrane. According to [33–35], the ratio C'/C should be most sensitive to the rotation of spin labels about the long axis, whereas the ratio L''/L should give the correlation time for the motion of the long axis itself. The ratio C'/C of the V_2' spectrum provides a reasonable approximation for the correlation time $\tau_\parallel$ ($\tau_R(C) \cong \tau_\parallel$) if $\tau_\parallel \ll \tau_\perp$ and $\tau_\parallel \ll \tau_R$, where the correlation time τ_R describes the overall motion of the membrane or macromolecular complex [33]. It also has been demonstrated that $\tau_R(L) \cong \tau_\perp$, provided the correlation time $\tau_\perp$ is short with respect to the correlation time τ_R, i.e. $\tau_\perp \ll \tau_R$. Therefore, the extent of the anisotropy of sub-millisecond rotations can be formally described by the ratio $\xi = \tau_R(L)/\tau_R(C)$.

To calculate $\tau_R(L)$ and $\tau_R(C)$ from the peak height ratios L''/L and C'/C, we used the calibration curves obtained by Horvath and Marsh [22] from the reference spectra of spin label tightly bound to hemoglobin in a water–glycerol mixture. Assuming that in the water–glycerol mixture, a hemoglobin molecule rotates almost isotropically, one could expect that the relationship $\tau_R(L) \approx \tau_R(C)$ should be fulfilled for radicals rotating isotropically in the membrane. Therefore, the essential deviation of the ratio $\xi = \tau_R(L)/\tau_R(C)$ from the 'isotropic' value $\xi = 1$ indicates the anisotropic character of the nitroxide radical rotation in the lipid membrane. For the spin label 5-SASL, whose doxyl group is located in the hydrocarbon region close to the headgroup region of the membrane, we found that the apparent anisotropy parameter $\xi \cong 18$ (Fig. 8C). This value is markedly higher than the anisotropy parameter ξ determined for the spin labels 12-SASL ($\xi \cong 5$) and 16-SASL ($\xi \cong 10$), the radicals of which are buried into the depth of the membrane. This result demonstrates that the flexibility profile along the lipid hydrocarbon chain does exist even at low temperatures, when most cell lipids are in solid state and the extent of ordering of the nitroxide radicals in the membrane surface region is essentially higher than in the depth of the membrane.

For the lipophilic methyl esters (*n*-MeSASL), the apparent correlation times $\tau_R(L)$ and $\tau_R(C)$, (Fig. 8B) and the anisotropy parameter ξ (Fig. 8C) only weakly depended on the position of the doxyl group along the hydrocarbon chain. The nitroxide radical

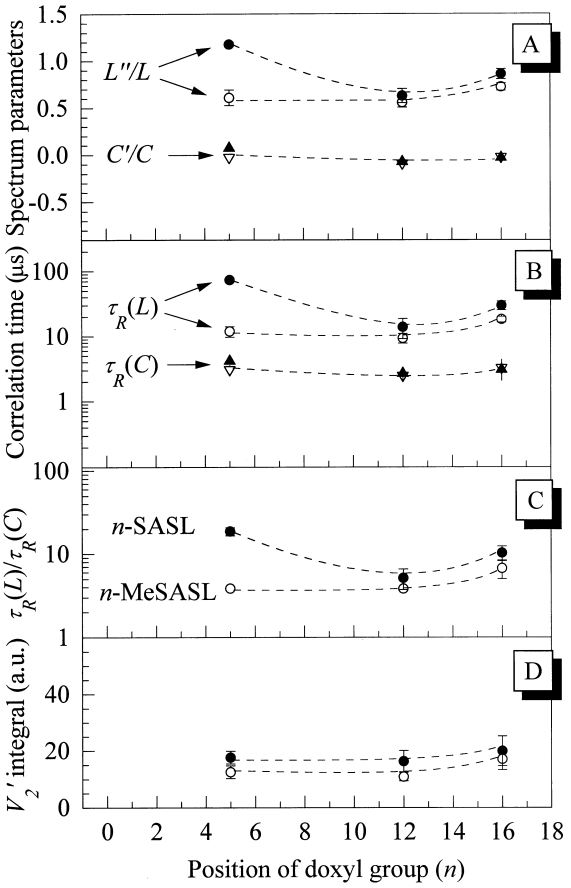

Fig. 8. Positional profiles of ST-EPR spectrum parameters L''/L and C'/C (A), the apparent correlation times $\tau_R(L)$ and $\tau_R(C)$ (B), anisotropy parameter $\xi = \tau_R(L)/\tau_R(C)$ (C) and integral intensity I_{ST} (D) of the ST-EPR signal from hydrated spin-labelled embryo axes. All spectra were recorded at −50°C. Solid symbols (circles and triangles) correspond to *n*-SASL, open symbols (circles and triangles) correspond to *n*-MeSASL.

of 5-MeSASL was less ordered in the membrane as compared with its amphiphilic analog 5-SASL. The nitroxide radicals of other pairs of spin label analogs (stearic acids and their methyl esters), corresponding to the same position of the doxyl group (12-SASL and 12-MeSASL, or 16-SASL and 16-MeSASL, respectively), showed similar mobility and anisotropy of rotation. Thus, we can conclude that nitroxide radicals of all the methyl ester spin labels remain disordered even at low temperatures, when all membrane lipids are in the gel phase. This result, along with the data presented in Section 3.3.1, suggests that methylated doxyl stearates are located predominantly in the core of bulk membrane lipids rather than in the protein boundary lipids.

The integral intensity of the V_2' spectrum, I_{ST}, is another parameter that is sensitive to the motion of nitroxide radicals in the sub-millisecond time-scale. According to [32–35], the value of I_{ST} increases with slowing down the rate of spin label rotation. The advantage of using the integral intensity is that parameter I_{ST} is relatively insensitive to small 'impurities' of weakly immobilized spin labels, being mainly determined by the rotation of the predominant portion of spin label molecules in a sample. For both kinds of spin label, *n*-SASL and *n*-MeSASL, parameter I_{ST} only weakly depended on the position of the doxyl group (Fig. 8D). It is remarkable that for *n*-SASL there was no correlation between positional profiles of I_{ST} and $\tau_R(L)$ and ξ. Indeed, the rotational correlation time $\tau_R(L)$ and anisotropy parameter ξ markedly decreased with deepening of the doxyl group of *n*-SASL from the position $n = 5$ to the position $n = 12$, whereas the integral intensity I_{ST} remained at the same level. Like $\tau_R(C)$, the integral intensity I_{ST} weakly depended on the doxyl group position in *n*-SASL. As we have mentioned above, $\tau_R(C)$ should be most sensitive to the spin label rotation around the long hydrocarbon chain of stearic acid. The relatively weak dependence of $\tau_R(C)$ and I_{ST} on the position of a nitroxide radical indicates that different spin-labelled derivatives of stearic acid perform axial rotations of similar rates. Therefore, we can conclude that high correlation time $\tau_R(L)$ of 5-SASL reflects the restricted degree of the hydrocarbon chain mobility (at the position $n = 5$) rather than the slowing down of the nitroxide radical rotation around the long chain of 5-SASL.

3.3.2.2. Spin labels in oil systems. Fig. 7 demonstrates ST-EPR spectra (at −50°C) of *n*-SASL and *n*-MeSASL dissolved in seed oil droplets and bulk seed oil, respectively. Fig. 9 shows the positional profiles of ST-EPR spectrum parameters. One can see that there was no essential difference between the spectra of stearic acids and their methylated derivatives labelled at the same position along the hydrocarbon chain (Fig. 9A). Therefore, SASLs and MeSASLs were characterized by similar profiles of $\tau_R(L)$ and $\tau_R(C)$ (Fig. 9B). On the other hand, the positioning of the doxyl group markedly influenced the shape of ST-EPR spectra, indicating that the nitroxide radicals of 16-SASL and 16-MeSASL rotate slowly (Fig.

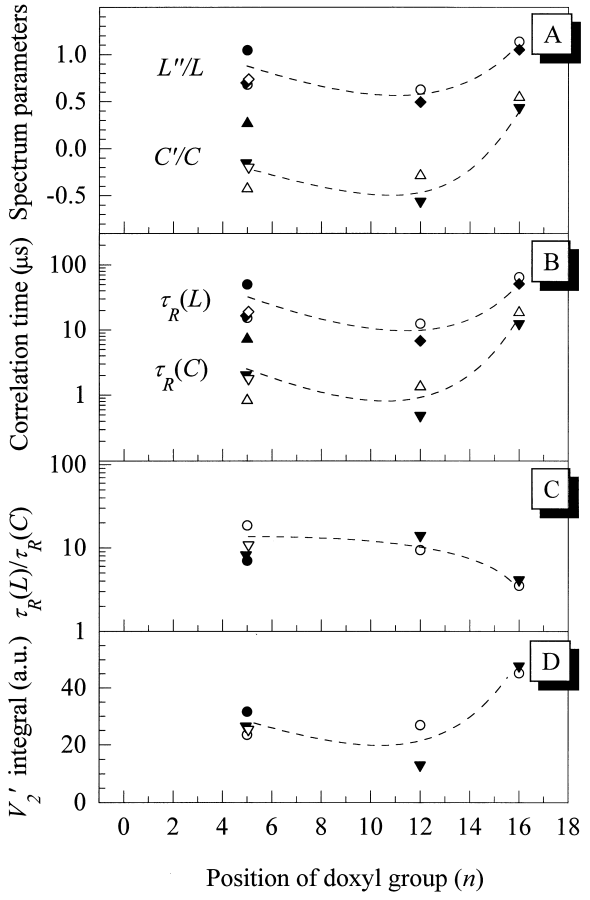

Fig. 9. Positional profiles of ST-EPR spectrum parameters L''/L and C'/C (A), the apparent correlation times $\tau_R(L)$ and $\tau_R(C)$ (B), anisotropy parameter $\xi = \tau_R(L)/\tau_R(C)$ (C) and integral intensity I_{ST} (D) of the ST-EPR signal from oil systems: *n*-SASL in oil droplets in water and *n*-MeSASL in bulk oil, respectively. All spectra were recorded at −50°C. Solid symbols correspond to *n*-SASL, open symbols correspond to *n*-MeSASL. Circles and triangles correspond to the preparations from wheat oil, diamonds and inverse triangles correspond to the preparations from purified sunflower oil.

9B) and much more isotropically (Fig. 9C), as compared with 5-SASL, 5-MeSASL, 12-SASL and 12-MeSASL. The rise of the apparent correlation times $\tau_R(L)$ and $\tau_R(C)$ (Fig. 9B) correlated with the increase in the integral intensity I_{ST} (Fig. 9D). Such an explicit dependence of the nitroxide radical mobility on the doxyl group position is likely to be the result of different conformations of doxyl stearate molecules caused, for example, by different apparent p*K* values of SASLs [36,37].

Comparing the positional profiles for spin labels in oil droplets (Fig. 9) with the relevant profiles for embryo axes (Fig. 8), one can see that at low temperatures both spin labels, 16-SASL and 16-MeSASL, rotate slowly and more isotropically in oil moiety than in axis cells. The essentially different profiles for axes and oil droplets suggest that most of the lipid soluble spin labels incorporated into axis cells is localized in axis cell membranes rather than in the interior of oil bodies. This is remarkable because the amount of neutral lipids in axes exceeds the amount of phospholipids by a factor of 5 [16]. However, it still remains possible that a certain part of the doxyl stearates had incorporated into the phospholipid monolayer that surrounds oil bodies [38]. Taking into account that the linear dimensions of lipid bodies are approximately 2 μm (unpublished data) and taking the thickness of the monolayer as 2 nm, we can estimate that the contribution of the phospholipid monolayers around the lipid bodies to the total of the membranes should be negligible (i.e. a few percent).

4. Conclusions

The present study demonstrates the possibility of in situ EPR spin-labelling technique to study plasma membranes of wheat embryo cells. Dynamic properties and structural organization of membranes in embryo axis cells were assayed with lipid soluble doxyl derivatives of stearic acid. We measured two kinds of EPR signals, conventional in-phase first derivative signal and out-of-phase second harmonics absorption signal, to analyze the ordering and mobility of nitroxide radicals in membranes. These spectra, recorded in the temperature interval from −50 to 20°C, were compared with the relevant EPR signals from lipid soluble spin labels dissolved in a suspension of droplets made of seed oil.

Spin labels of two kinds, stearic acid derivatives and their methylated analogs, that differ in their affinity to proteins, allow probing of the physical state of bulk membrane lipids and protein boundary lipids. Analysing the EPR spectrum parameters versus the position of the paramagnetic doxyl group along the hydrocarbon chain of stearic acid, we conclude that the vast majority of spin label molecules accumulated in the embryo axis is located in cell membranes rather than in the interior of lipid bodies. This

conclusion follows from the comparison of positional profiles in an embryo axis and a model oil system.

Acknowledgements

We would like to thank Professor Enno K. Ruuge for valuable support of this work and helpful discussions, Dr. Boris V. Trubitsin for his software used in this work to collect and process EPR data and Dr. Alexander A. Timoshin for technical assistance. This work was supported in part by Grant 047.01.006.96 from the Dutch Organization for Scientific Research and Grant 00-04-48330 from the Russian Foundation for Basic Researches.

References

[1] D. Chapman, E. Oldfield, Methods Enzymol. 32 (1974) 198–211.
[2] L.J. Berliner (Ed.), Spin Labeling: Theory and Applications, Academic Press, New York, 1976.
[3] J.H. Crowe, F.A. Hoekstra, L.M. Crowe, Annu. Rev. Physiol. 54 (1992) 579–599.
[4] W.F. Wolkers, M. Alberda, M. Koornneef, K.M. Léon-Kloosterziel, F.A. Hoekstra, Plant J. 16 (1998) 133–143.
[5] F.A. Hoekstra, C. Bomal, F.A.A. Tetteroo, in: D. Côme, F. Corbineau (Eds.), Proceedings of the Fourth International Workshop on Seeds: Basic and Applied Aspects of Seed Biology, Angers, France, 20–24 July, 1992, ASFIS, Paris, 1993, pp. 755–762.
[6] D. Marsh, in: E. Grell (Ed.), Membrane Spectroscopy, Springer, Berlin, 1981, pp. 51–142.
[7] P.D. Morse, II, in: G. Benga (Ed.), Structure and Properties of Cell Membranes, vol. 3, CRC Press, Boca Raton, FL, 1985, pp. 195–236.
[8] D. Marsh, in: P.M. Bayley, R.E. Dale (Eds.), Spectroscopy and the Dynamics of Molecular Biological Systems, Academic Press, London, 1985, pp. 209–238.
[9] N. Kocherginsky, H.M. Swartz, Nitroxide Spin Labels, Reactions in Biology and Chemistry, CRC Press, New York, 1995.
[10] J.F.W. Keana, S. Pou, Physiol. Chem. Phys. Med. NMR 17 (1985) 235–240.
[11] F. Kamp, D. Zakim, N. Noy, J.A. Hamilton, Biochemistry 34 (1995) 11928–11937.
[12] D.O. Nettelton, P.D. Morse II, J.W. Dobrucki, H.M. Swartz, N.J.F. Dodd, Biochim. Biophys. Acta 944 (1988) 315–320.
[13] L.B. Margolis, A.N. Tikhonov, E.Yu. Vasilieva, Cell 19 (1980) 189–195.
[14] V.A. Tverdislov, A.N. Tikhonov, L.V. Yakovenko, Physical Mechanisms of Biological Membranes Functioning, Moscow University Press, Moscow, 1987, pp. 73–84 (in Russian).
[15] E.A. Golovina, A.N. Tikhonov, Biochim. Biophys. Acta 1190 (1994) 358–392.
[16] E.A. Golovina, A.N. Tikhonov, F.A. Hoekstra, Plant Physiol. 114 (1997) 343–348.
[17] R.C. MacDonald, R.I. MacDonald, B.P.M. Menco, K. Takeshita, N.K. Subbarao, L. Hu, Biochim. Biophys. Acta 1061 (1991) 297–303.
[18] B.V. Trubitsin, Yu.A. Koksharov, N.A. Shatalov, E.K. Ruuge, A.N. Tikhonov, in: Proceedings of the Xth International Conference 'Magnetic Resonance in Chemistry and Biology', Suzdal, Russia, 1998, p. 9.
[19] T.C. Squier, D.D. Thomas, Biophys. J. 49 (1986) 921–935.
[20] D. Marsh, K. Schorn, in: L. Berliner (Ed.), Biological Magnetic Resonance, vol. 14, Spin Labelling: the Next Millenium, Plenum Press, New York, 1998, pp. 405–410.
[21] B.J. Gaffney, in Spin Labeling. Theory and Applications (L.J. Berliner, Ed.), Academic Press, New York, 1976, p. 567.
[22] L.I. Horvath, D. Marsh, J. Magn. Res. 54 (1983) 363–373.
[23] C.A. Evans, J. Magn. Res. 44 (1981) 109–116.
[24] G. Zaccai, G. Buildt, A. Seelig, J. Seelig, J. Mol. Biol. 134 (1979) 693–706.
[25] E.A. Vishnyakova, A.E. Ruuge, E.A. Golovina, F.A. Hoekstra, A.N. Tikhonov, Biochim. Biophys. Acta, submitted for publication.
[26] D. Chapman, R.M. Williams, B.D. Ladbrook, Chem. Phys. Lipids 1 (1967) 445–475.
[27] J.H. Crowe, L.M. Crowe, in: F. Franks (Ed.), Water Science Reviews, vol. 5, Cambridge University Press, Cambridge, 1990, pp. 1–23.
[28] J.S. Hyde, D.D. Thomas, Ann. N. Y. Acad. Sci. 222 (1973) 680–692.
[29] D.D. Thomas, R.L. Dalton, J.S. Hyde, J. Chem. Phys. 65 (1976) 3006–3024.
[30] J.S. Hyde, L.R. Dalton, in: L.J. Berliner (Ed.), Spin Labeling II. Theory and Applications, Academic Press, New York, 1982, pp. 1–70.
[31] M.A. Hemminga, Chem. Phys. Liquids 32 (1983) 323–383.
[32] D. Marsh, L.I. Horvath, in: A.J. Hoff (Ed.), Advanced EPR. Applications in Biology and Biochemistry, Elsevier, Amsterdam, 1989, p. 707.
[33] M.A. Hemminga, P.A. de Jager, in: L.J. Berliner, J. Rueben (Eds.), Biological Magnetic Resonance, vol. 8, Spin Labeling. Theory and Applications, Plenum Press, New York, 1989, pp. 131–176.
[34] D. Marsh, Biochemistry 19 (1980) 1632–1637.
[35] P. Fajer, D. Marsh, J. Magn. Res. 51 (1983) 446–459.
[36] A. Sanson, M. Ptak, J.L. Rigaud, C.M. Gary-Bobo, Chem. Phys. Lipids 17 (1976) 435–444.
[37] A. Kusumi, W.K. Subczynski, J.S. Hyde, Fed. Proc. 41 (1982) 1394, Abstr. 6571.
[38] J.T.C. Tzen, A.H.C. Huang, J. Cell Biol. 117 (1992) 327–335.